Journal of Visualized Experiments

Application of Ultrasound and Shear Wave Elastography Imaging in a Rat Model of NAFLD/NASH

--Manuscript Draft--

Article Type:	Invited Methods Article - JoVE Produced Video
Manuscript Number:	JoVE62403R1
Full Title:	Application of Ultrasound and Shear Wave Elastography Imaging in a Rat Model of NAFLD/NASH
Corresponding Author:	Dinesh Kumar Hirenallur Shanthappa, BVSc, MVSc, PhD, DACLAM Pfizer Inc Cambridge, MA UNITED STATES
Corresponding Author's Institution:	Pfizer Inc
Corresponding Author E-Mail:	DineshH@pfizer.com
Order of Authors:	Jeffrey Morin
	Terri Swanson
	Anthony Rinaldi
	Magalie Boucher
	Trenton Ross
	Dinesh Kumar Hirenallur Shanthappa, BVSc, MVSc, PhD, DACLAM
Additional Information:	
Question	**Response**
Please indicate whether this article will be Standard Access or Open Access.	Standard Access (US$2,400)
Please specify the section of the submitted manuscript.	Biology
Please indicate the **city, state/province, and country** where this article will be **filmed**. Please do not use abbreviations.	Cambridge, MA, USA
Please confirm that you have read and agree to the terms and conditions of the author license agreement that applies below:	I agree to the Author License Agreement
Please provide any comments to the journal here.	
Please indicate whether this article will be Standard Access or Open Access.	Standard Access ($1400)

TITLE:

Application of Ultrasound and Shear Wave Elastography Imaging in a Rat Model of NAFLD/NASH

AUTHORS AND AFFILIATIONS:

Jeffrey Morin[1*], Terri A. Swanson[2*], Anthony Rinaldi[3], Magalie Boucher[4], Trenton Ross[3], Dinesh Hirenallur Shanthappa[1]

[1]Comparative Medicine, Pfizer Inc., Cambridge, MA, USA
[2]Digital Medicine & Translational Imaging, Pfizer Inc., Cambridge, MA, USA
[3]Internal Medicine Research Unit, Pfizer Inc., Cambridge, MA, USA
[4]Drug Safety Research & Development, Pfizer Inc., Cambridge, MA, USA

*These authors contributed equally.

Email addresses of co-authors:

Jeffrey Morin	(jeffrey.morin@pfizer.com)
Terri Swanson	(terri.a.swanson@pfizer.com)
Anthony Rinaldi	(anthony.rinaldi@pfizer.com)
Magalie Boucher	(magalie.boucher@pfizer.com)
Trenton Ross	(trenton.ross@pfizer.com)

Corresponding author:

Dinesh Hirenallur-Shanthappa (dineshh@pfizer.com)

KEYWORDS:

Nonalcoholic Fatty Liver Disease (NAFLD), steatosis, nonalcoholic steatohepatitis (NASH), liver fibrosis, shear wave elastography, liver ultrasound

SUMMARY:

This protocol describes the use of an enhanced ultrasound technique to non-invasively observe and quantify liver tissue changes in rodent models of nonalcoholic fatty liver disease.

ABSTRACT:

Nonalcoholic Steatohepatitis (NASH) is a condition within the spectrum of Non-Alcoholic Fatty Liver Disease (NAFLD), which is characterized by liver fat accumulation (steatosis) and inflammation leading to fibrosis. Preclinical models closely recapitulating human NASH/NAFLD are essential in drug development. While liver biopsy is currently the gold standard for measuring NAFLD/NASH progression and diagnosis in the clinic, in the preclinical space, either collection of whole liver samples at multiple timepoints during a study or biopsy of liver is needed for histological analysis to assess the disease burden.

Conducting a liver biopsy mid-study is an invasive and labor-intensive procedure, and collecting liver samples to assess disease level increases the number of research animals needed for a study. Thus, there is a need for a reliable, translatable, non-invasive imaging biomarker to detect

NASH/NAFLD in these preclinical models. Non-invasive ultrasound-based B-mode images and Shear Wave Elastography (SWE) can be used to measure steatosis as well as liver fibrosis. To assess the utility of SWE in preclinical rodent models of NASH, animals were placed on pro-NASH diets and underwent non-invasive ultrasound B-mode and shear wave elastography imaging to measure hepatorenal (HR) index and liver elasticity, measuring progression of both liver fat accumulation and tissue stiffness, respectively, at multiple time points over the course of a given NAFLD/NASH study.

The HR index and elasticity numbers were compared to histological markers of steatosis and fibrosis. The results showed strong correlation between the HR index and percentage of Oil Red O (ORO) staining, as well as between elasticity and Picro-Sirius Red (PSR) staining of livers. The strong correlation between classic *ex vivo* methods and *in vivo* imaging results provides evidence that shear wave elastography/ultrasound-based imaging can be used to assess disease phenotype and progression in a preclinical model of NAFLD/NASH.

INTRODUCTION:

Non-alcoholic fatty liver disease (NAFLD) is a metabolic condition characterized by an excessive buildup of fat in the liver and is quickly becoming a leading liver ailment worldwide with a recently reported global prevalence of 25%[1]. Non-alcoholic steatohepatitis (NASH) is a more progressed stage of the spectrum of NAFLD, characterized by excess liver fat with progressive cellular damage, fibrosis, and inflammation. These ailments are often silent, undetected via blood tests or routine examinations, until considerable damage has already occurred to a patient's liver. Currently, the gold standard to diagnose NASH in patients is through histological examination of patient-derived liver biopsy samples. Similarly, preclinical researchers who work to understand the pathogenesis of NASH/NAFLD as well as the drug development industry rely on *in vivo* wedge biopsy of liver samples or terminal euthanasia of satellite cohorts for histology to measure steatosis, inflammation, and fibrosis.

For example, liver wedge biopsy has been a standard technique for assessing steatohepatitis and fibrosis while using the GUBRA NASH model[2]. The liver wedge biopsy method is invasive and laborious in small animals[3]. The use of wedge liver biopsy in the middle of a study represents an added experimental variable in a disease model, which often increases the number of animals that are needed. With these factors in mind, non-invasive imaging techniques that can be used to reliably assess steatosis and fibrosis in NASH/NAFLD animal models at early time points prove valuable. Shear wave elastography (SWE) is an ultrasound-based method used to measure the elasticity of soft tissues. The technique measures the propagation of shear waves created by supersonic ultrasound pulses directed at a tissue target, and then calculates a value called E modulus[4]. The velocity of the shear wave is proportional to the degree of tissue stiffness.

Figure 1 and **Figure 2** show the imaging area setup and the SWE instrument. The SWE instrument is a single, wheeled unit with two screens and a control panel shown in **Figure 2A**. The upper monitor (**Figure 2B**) acts as the computer monitor and displays images and patient directories. The control panel (**Figure 2C**) is an array of buttons and dials that control general aspects of image capture: freezing screen, saving images, changing from one mode to another. The lower screen

(**Figure 2D**) is a touch screen with additional controls to change settings and acts as a keyboard to input data as needed. The instrument is equipped with a stylus to use on the touch screen if desired. Ultrasound probes attach to the lower front panel of the device. For B-mode and SWE imaging in rodents, the super-linear 6 to 20 MHz transducer was used. This ability to noninvasively measure tissue stiffness makes SWE a valuable tool for the identification and staging of liver fibrosis[5] in NASH patients, decreasing the need for more invasive methods. SWE has, in fact, been used to measure liver fibrosis in patients and is an FDA-approved method to score fibrosis in the clinic[6]. Using SWE to monitor NASH progression in animal models of the disease would provide a translational tool for the development of treatments and simultaneously improve animal welfare through the reduction of animal subject numbers and refinement of *in vivo* procedures to minimize pain and distress.

SWE imaging in human patients uses a low-frequency ultrasound transducer[4], which is not ideal for small animals. Notably, high-frequency SWE techniques have been used to evaluate the efficacy of acetyl-CoA carboxylase inhibition on pathogenesis of NASH in a rat model[7], and the utility of this technique has been described in carbon tetrachloride rat models of liver fibrosis with successful results when compared to traditional METAVIR histological scoring methods[8]. However, existing literature lacks detailed technique and methodology information on the application of SWE imaging in preclinical models of NASH. As described above, liver steatosis is one of the key features of the NAFLD/NASH condition and is an important stage where intervention can be considered. Thus, assessing liver fat accumulation using an imaging modality is as important as assessing liver fibrosis in preclinical models of NASH/NAFLD.

An ultrasound technique known as the HR index, a ratio of tissue brightness of the liver compared to that of the renal cortex, has been used as a surrogate marker of steatosis in the clinic[9,10]. This approach, however, has not been extensively used in preclinical animal models of NAFLD/NASH. This article describes a method of measuring elasticity as well as the HR index as a surrogate marker of hepatic fibrosis and steatosis, respectively, in a choline-deficient, high-fat diet (CDAHFD) rat model of NAFLD/NASH. This model induces rapid steatosis, liver inflammation, and fibrosis, which is measurable within 6 weeks in mice[11]. The addition of cholesterol (1%) to this diet has been shown to improve fibrogenesis in rats[12], making this model a suitable candidate for validation studies involving shear wave imaging. Overall, this imaging technology can also be applied to a wide range of NASH models/diets where steatosis and/or fibrosis is an endpoint of interest.

PROTOCOL:

All animal-involved procedures were reviewed and approved by Pfizer's Institutional Animal Care and Use Committee (IACUC) and conducted in an AAALAC (Assessment and Accreditation of Laboratory Animal Care) International accredited facility.

1. Disease induction

1.1. Use male Wister Han rats (150–175 g; ~ 6–7 weeks old; total 40 rats) that are free of

known rat adventitial pathogens. House the rats in pairs in individually ventilated caging with paper bedding (see the **Table of Material**s) and maintain them at 22 ± 1 °C, 40–70% relative humidity with a 12:12 h light-dark cycle.

1.2. Place the rats weighing 150–175 g (~6–7 weeks old) on a choline-deficient, high-fat diet with 1% cholesterol (n = 20) or a standard lab rodent chow (n = 20) depending on the study design.

NOTE: In this study, a total of 40 rats were enrolled with 20 animals per group. At the end of the 6th week, half of the cohort from each group was necropsied for mid-study histological analysis of liver samples. Thus, the sample size was 10 animals per group for 9th and 12th week time points.

2. Instrument setup

2.1. Set up the imaging area as follows: include a warmed surface to keep the animal warm during imaging (c in **Figure 1**), and a secured anesthesia nose cone to deliver inhalant anesthesia to maintain a plane of anesthesia throughout the procedure (b in **Figure 1**).

2.2. Use an ultrasound probe holder to facilitate moving the ultrasound probe to the desired location and to prevent the probe from resting on the animal.

2.2.1. Use warmed ultrasound gel on the skin where the ultrasound image is acquired.

2.2.2. Maintain the following settings throughout the procedure, which can be adjusted on the touch screen: Acoustic Power 0.0 dB; Tissue Tuner 1540 m/s; Dynamic Range 60 dB; Elasticity range (for SWE mode) < 30 kPa.

2.3. Attach the ultrasound probe to the rail system in the specialized holder (a in **Figure 1**).

2.4. Switch the instrument on and allow it to boot up. Once the monitor is turned on, note the **B Mode** image with connected transducer details.

3. Subject preparation

3.1. Make sure the animals are fasted at least 4 h prior to the imaging procedure to prevent gut content from interfering with image acquisition.

3.1.1. After at least 4 h of fasting, place a rat in an isoflurane anesthetic induction chamber until a suitable level of anesthesia is reached, confirmed by no response to toe pinch. Expose the animals to 3–5% isoflurane for 3–5 min to induce anesthesia.

3.1.2. For maintenance anesthesia, keep the animals under 2–3% isoflurane during image acquisition. Apply ophthalmic ointment to protect the eye from drying during anesthesia.

3.2. Once anesthesia has been achieved, remove an animal from the induction chamber and place it on a warm hot water circulating blanket. Place an anesthetic nose cone over the snout, and shave the animal on its right side, from the ribcage to pelvis. Use chemical depilation cream to remove all the remaining hair in this area.

3.3. Once hair has been removed, place an animal in left lateral recumbency with upper paws taped above the head on a warm imaging platform (**Figure 3A**).

3.4. Press the **Patient** key on the instrument control panel, and identify the subject according to the study design.

3.4.1. Open the **Keyboard** function on the instrument by tapping the icon on the touch screen. Type the names as desired.

3.4.2. Tap **Exit** to exit the patient name screen. Observe that B-mode reopens on the monitor.

4. Image acquisition for hepato-renal (HR) index measurement

4.1. Apply a small amount of warmed ultrasound gel to the depilated skin region on the animal.

4.2. Move the ultrasound probe to touch the gel-covered area of the subject (**Figure 3B**). Once a live B-mode image of the subject's internal organs appears on the monitor, move the ultrasound probe to the area slightly above the hip, just parallel to the lumbar vertebrae (sagittal plane).

4.3. Using the B-mode display on the monitor, locate the right kidney by identifying the large renal artery and cortex/medulla separation (**Figure 4A**). In addition, observe part of the liver in a single plane of the image.

4.3.1. Ensure that there are little to no image artifacts such as shadows and air bubbles.

4.4. Measure a B Mode ratio to obtain the HR index.

4.4.1. Ensure that both renal cortex and liver parenchyma are in the same plane of focus. If needed, adjust focus and gain control to obtain a clear image.

4.4.1.1. Adjust the focus by turning the **Focus** knob on the control panel. Adjust the gain by pressing the **Auto TGC** button once.

4.4.2. Press the **Freeze** key on the control panel. Ensure that the animal is between breaths when freezing the screen to avoid blurry images.

4.4.3. Once the screen is frozen, tap **Measurement Tools** on the touch screen. Select **B-mode**

Ratio, a built-in tool that measures relative brightness of a tissue from a selected region of interest. Create a 2 mm circle to select a region of interest (ROI). Adjust the circle size by moving a finger along the outer edge of the trackball on the control panel.

4.4.4. Place the 2 mm circle on the liver image ROI, which should be located to the right of the kidney. Identify liver tissue based on its homogeneous echogenicity and smooth contour.

4.4.5. Once the circle is in place, press the **Select** button on the control panel, and observe the new circle that appears.

4.4.6. Adjust the size of the new circle to 2 mm, and place it on the image of the kidney cortex. Be sure to keep the depth of the circles on the liver and kidney cortex the same. Once in place, press the **Select** button on the control panel. Observe how the built-in system tool displays the HR index as a B-mode ratio.

4.4.7. Press **Save Image** to save the image, and observe the saved images that appear as thumbnails on the right side of the monitor.

4.4.8. Press the **Freeze** button on the control panel to unfreeze the image and return to a live B mode image.

4.5. Repeat the B Mode ratio measurement 3 times at different depths and planes of tissue. Calculate the average of these three B-mode ratios for each animal and time point.

5. Image acquisition for Shear Wave Elastography

5.1. Move the probe transversely in the right subcostal area to locate the liver using B Mode. Locate an area of the liver that is mostly parenchyma and free of large blood vessels such as the portal vein and hepatic artery. Once a clear area of the liver has been found, generate a shear elasticity map of the tissue by pressing the **SWE** button on the control panel.

5.2. Adjust the size and position of the SWE box below the liver capsule in an area that is free of shadows. Identify the capsule as a bright echogenic line near the top of the liver.

5.3. Observe that the SWE box transitions to a color map within 5–10 s. Once the box is full and stable, press the **Freeze** button on the control panel when the animal is between breaths.

NOTE: The minimum amount of box coverage should be 60–80% to accurately assess the elasticity of the liver.

5.4. On the touch screen, tap **QBox**, a built-in system tool that computes elasticity from an ROI on the shear wave elasticity map. Observe the circle and data box that appear on the monitor. Adjust the position of the QBox by tapping the position icon on the touch screen to the desired setup.

5.5. Adjust the size of the circle to 3 mm by moving a finger along the outer edge of the trackball on the control panel. Using the trackball, position the circle in an area free from shadow with uniform coloring (**Figure 5A,B**). Take care to avoid known areas of stiffness such as blood vessels or the liver capsule, as well as bleed-down from these structures.

5.6. When an adequate area is found, press **Save Image** on the control panel to save the image. Repeat this procedure 3 times in different areas of the liver. Move the probe up and down or sideways on the abdomen to gather SWE-mapped images from different areas of the liver.

5.7. Once all images have been collected, press **End Exam** on the control panel, and make note of the patient information screen that appears on the monitor.

5.8. Remove the tape from the animal's paws, wipe excess gel away, and remove the animal from the imaging stage. Allow it to recover from anesthesia in a warm, dry cage by itself until fully recovered. Monitor each animal to ensure full recovery from anesthesia, indicated by its ability to maintain sternal recumbency

5.9. Repeat steps in sections 4–5 for each animal in the cohort to be imaged.

6. Image data retrieval and analysis

6.1. When images for all animals have been collected, turn off the anesthesia.

6.2. To pull image data from the machine, press the **Review** button on the control panel, and observe all the scans performed on that instrument that appear on the monitor. Search for the desired scans using the search window in the upper corner of the screen.

6.3. Select all scans needed for data analysis by checking the box next to the name of the patient via the trackball and **Select** button. Once all needed scans are highlighted, select **Export JPEGs** on the touch screen. Export data to a network drive or a portable Universal Serial Bus (USB) drive. Locate the USB ports on the back of the instrument.

6.4. Once the files have been exported, open individual jpg files of each scan on a workstation computer. Observe all the data on the right side of the image: B Mode Ratio—collect the B Ratio number; Q Box—collect the mean elasticity (kPa) value.

6.5. Enter all data into a spreadsheet or other database management software, and perform the desired statistical analyses.

7. Histological analysis of liver samples

7.1. At the end of the 6th week, perform necropsy on half of the cohort from each group for mid-study histological analysis of the liver samples. Similarly, euthanize the rest of the cohort of

animals, and collect liver samples for histological analysis at the 12th week time point.

7.2. For ORO staining, fix liver sections in 10% neutral-buffered formalin, and cryopreserve them with sucrose using a refrigerated 30% sucrose solution overnight at a minimum. Cryo-embed the sections in optimal cutting temperature compound, and cryo-section them onto charged slides to prepare for ORO staining.

7.3. Place the cryo-sections in 100% propylene glycol for 2 min followed by an overnight incubation in 0.5% ORO solution. After removal from the ORO solution, differentiate the sections in 85% propylene glycol for 1 min, rinse in deionized water, and counterstain with Mayer's Hematoxylin—Lillie's modification for 1 min.

7.3.1. Place coverslips on the slides using an aqueous mounting medium and dry them at room temperature.

7.4. For PSR, deparaffinize formalin-fixed, paraffin-embedded liver section slides, place them overnight in Bouin Fluid, and then stain them using an automated slide stainer as per the manufacturer's protocol with some optimized steps (1% phosphomolybdic acid for 5 min; 0.1% Sirius Red in saturated picric acid for 90 min; 2 x 30 s wash in 0.5% acetic acid). Automatically dehydrate the slides and then mount them with a permanent mounting medium.

7.5. Capture images of the ORO- and PSR-stained slides using the digital microscopy scanner at 20x magnification, save them in .svs format, and store in the slide manager image database.

7.6. Analyze the images using custom algorithms created in digital pathology software. Uniformly apply digital pathology software applications with threshold parameters to identify and quantify the liver sections area as well as the ORO- and PSR-stained areas. Export the measurements to a spreadsheet for area percentage calculations.

8. Statistical analysis

8.1.1. Perform statistical analysis of the imaging data with two-way ANOVA using Sidak's multiple comparisons test to assess the difference between groups at different time points. Assume significant differences between groups for probability values $p \leq 0.001$. In addition, perform correlation of imaging readouts with histological analyses.

8.1.2. Use non-parametric statistics to analyze the histological analysis results from this study. Report the group values as median ± semi-interquartile range (sIQR). Assume significant differences between groups for probability values $p \leq 0.001$. Use a Mann-Whitney test to compare the quantity of PSR and ORO histochemical stain between different groups.

REPRESENTATIVE RESULTS:

One hallmark of animals fed CDAHFD is steatosis. Accumulation of fat in the liver changes the echogenic properties of the tissue, which can be quantified by measuring the brightness of the

liver and normalizing it to the brightness of the renal cortex from a B-mode image taken in the same plane. The quantified value is expressed as an HR index, which is an indirect measure of steatosis. In **Figure 4A**, a representative liver image from a control animal shows approximately equal or less brightness (echogenicity) compared to the renal cortex. Thus, the HR index of normal animals is <1. In this study, the average HR index of control animals at the 3-week time point is 0.645 ± 0.03. In contrast, a representative B-mode image of a CDAHFD-fed animal (**Figure 4A**) shows increased brightness of the liver compared to the renal cortex. As a result, the HR indices of representative images from the CDAHFD diet animals were 1.91 and 1.79 at the 6- and 12-week time points, respectively.

Figure 4C shows a plot of HR indices over time from control and CDAHFD animals. Control-diet-fed animals show little movement in HR index values from baseline, whereas CDAHFD animals rise quickly over the course of the first 3–6 weeks of the study before reaching a plateau. The average HR index of animals that were on a CDAHFD diet is 1.861 ± 0.06 compared to 0.328 ± 0.03 in control animals at 12 weeks post-disease induction. As expected, the liver showed a significantly higher positive percent area for ORO staining in the CDAHFD group compared to the control diet group at 6- (34.81 ± 4.66 vs. 0.49 ± 0.11) and 12- (30.08 ± 2.64 vs. 1.17 ± 0.44) week time points (**Figure 4B,D**). There was also excellent correlation (Pearson r = 0.78) between the percent area of ORO staining with the HR index at the 6- and 12-week time points (**Figure 4E**). These results suggest the HR index can be a valuable imaging readout to quantify steatosis in preclinical models of NAFLD/NASH.

One of the key elements of measuring liver stiffness via SWE is proper placement of the ROI (**Figure 5**). The left panel (**Figure 5A**) shows a representative image with B-mode and SWE mapping of liver from a control diet animal. Proper ROI placement should be over an area that is stable in the color map and represents the section of the liver being measured, with a signal that is not influenced by adjacent structures such as the liver capsule and blood vessels. Tissue stiffness is reported as the E modulus, which is a calculation based on shear wave speed and a determined constant and is expressed in kilopascals (kPa). For control animals, the E modulus falls between 3.5 kPa and 6 kPa. The mean kPa of the ROIs reported in **Figure 5A** for control animals were 4.6 and 5.5 kPa at the 6- and 12-week time points, respectively, which falls within the expected normal range. **Figure 5A** shows a representative image of the SWE mode from a CDAHFD animal at 6 and 12 weeks. Here, the ROI has again been placed near the center of the Q Box (shear wave map), based on the colored reference on top of the image.

As expected with this model, the E modulus is much higher in the CDAHFD-fed animal. In these representative images, the mean kPa was 10.5 at 6 weeks and 23.1 kPa at 12 weeks, indicating significant tissue stiffness. A typical NASH diet study utilizing CDAHFD and control chow should reveal a steady progression of liver stiffness due to fibrosis in the CDAHFD-fed animals, while control animals remain the same. **Figure 5C** shows a gradual increase in elasticity of the liver in CDAHFD animals compared to stable elasticity in control animals over a 12-week period. Control diet elasticity starts at 5.80 ± 0.99 kPa at the 3-week time point and does not display much change (6.14 ± 0.59) over the course of the 12-week study. The choline-deficient diet, however, shows a significant increase quite early, reaching 12.07 ± 2.37 kPa by week 6. The trend in increased

elasticity continues in the CDAHFD diet as the study progresses, reaching 24.43 ± 9.29 kPa at 12 weeks post-special diet initiation.

Liver samples were stained with PSR to localize collagen as a correlate of fibrosis. As expected with this model, there is a significantly higher percentage of liver PSR-positive staining observed in CDAHFD animals compared to the control diet at both 6- and 12-week time points (**Figure 5D**). To establish the utility of the shear wave as a surrogate method to *ex vivo* staining, shear wave E Modulus numbers were plotted against the PSR-stained area in CDAHFD rats in **Figure 5E** to determine the correlation. Analysis of the plot revealed a tight cluster with a Pearson 'r' value of 0.88, indicating strong correlation. It should be noted that the results reported here are representative of what would be expected in a study using a choline-deficient, high-fat diet to induce NASH. This method can also be used with other preclinical NASH models; however, it will produce different results and cut-off values depending on the disease induction protocol. Like the rat NASH model, the SWE imaging in the CDAHFD-induced NASH mouse model showed excellent correlation between liver elasticity values and the percentage of PSR-positive stained area in liver[13]. Thus, SWE can be a valuable tool to assess liver fibrosis in preclinical models of NAFLD/NASH.

FIGURE AND TABLE LEGENDS:

Figure 1: Imaging setup. The ultrasound transducer (a) is held by the descending arm. The imaging stage (b) has an area to clamp the anesthesia hose and set up a nose cone (c) for continuous anesthesia during imaging. The stage is also heated and equipped with probes to monitor body temperature.

Figure 2: The Shear Wave Elastography instrument. (**A**) The shear wave elastography instrument is a single, wheeled unit with attachment ports for up to 4 ultrasound probes. (**B**) The upper monitor serves as the visual output for real-time viewing of images, as well as displaying patient data and system inventory. (**C**) The central control panel contains most of the buttons and knobs needed to adjust display and acquire images. (**D**) The lower monitor is a touch screen with additional controls and commands for image acquisition and adjustment.

Figure 3: Animal positioning and proper transducer placement. (**A**) Once an animal has been properly placed on the stage and restrained with tape-in left lateral recumbency (**B**) the ultrasound probe is lowered onto the rat, touching the gel placed on the abdomen/side. When the probe is touching the gel in the position in panel **B**, the kidney and liver can be seen in juxtaposition on the monitor. This is an optimal position to collect the hepato-renal index, and in some cases, the shear wave numbers as well.

Figure 4: Hepato-renal index results. (**A**) Representative image of HR indices from control and CDAHFD diet rats at 6- and 12-week time points. ROIs (red) were drawn in the kidney (left circle) and liver (right circle), then a ratio of the signals was determined (B Ratio, right data table). (**B**) Representative ORO-stained histological sections of liver samples from control and CDAHFD diet rats at 6- and 12-week time points. Scale bars = 300 μm. (**C**) Graphical representation of the HR

index over a disease-inducing diet time course. Control rat data are represented in blue, CDAHFD rat data in red. The graph shows mean values with standard error of the mean (n = 20 at the 3-week time point and n = 20 for control and n= 19 for CDAHFD at 6 weeks, n = 10 at 9- and 12-week time points (comparing control versus CDAHFD at each time point *, **, ***, ****p < 0.001). (**D**) Liver ORO calculations plotted for each time point (n = 10). The graph shows median values with interquartile range (*, ** p < 0.001). (**E**) Correlation graph comparing percent liver ORO-positive area versus the HR index. Abbreviations: HR = hepato-renal; CDAHFD = choline-deficient, high-fat diet; ROIs = regions of interest; ORO = Oil Red O.

Figure 5: Shear wave elastography results. (**A**) Representative image of SWE maps from control and CDAHFD diet rats at 6- and 12-week time points. ROIs (red) were drawn in the kidney (left circle) and liver (right circle), then a ratio of the signals was determined (B Ratio, right data table). (**B**) Representative ORO-stained histological sections of liver samples from control and CDAHFD diet rats at 6- and 12-week time points. The Scale bar on histological sections is 300 µm. (**C**) Graphical representation of liver tissue stiffness in a 12-week-diet-induced NASH rat model. Groups were fed normal chow (blue) or choline-deficient, high-fat diet (red) (n = 20 at 3 and 6 weeks, n = 10 at 9- and 12-week time points). The graph shows mean values with standard error of the mean (n = 20 at 3 and 6 weeks, n = 10 at 9- and 12-week time points (comparing control versus CDAHFD at each time point *, **, *** p < 0.001). (**D**) Graphical representation of collagen distribution in *ex vivo* histologic liver samples using collagen-specific PSR stain (n = 10). The graph shows median values with interquartile range (*, ** P < 0.001) (**E**) Linear regression graph comparing percent positive liver PSR staining area versus SWE elasticity. SWE = shear wave elastography; CDAHFD = choline-deficient, high-fat diet; ROIs = regions of interest; ORO = Oil Red O; NASH = nonalcoholic steatohepatitis; PSR = Picro Sirius Red.

DISCUSSION:

Ultrasound-based imaging, including SWE, can be an invaluable tool for the longitudinal assessment of liver steatosis and stiffness in preclinical models of NAFLD/NASH. This paper describes detailed methodologies on how to acquire high-quality B-mode as well as SWE images of livers for the measurement of the HR index and elasticity using a CDAHFD diet-induced rat model of NASH. Further, the results show excellent correlation of the HR index and elasticity with the gold standard of evaluation—histological assessment of liver tissue. While the procedure itself appears to be uncomplicated, there are some critical aspects of the protocol that will ensure successful outcomes.

The placement of the transducer is key, especially when looking for the kidney to measure the HR index in B-mode. Placing the probe too close to the ribs can result in rib shadow, which creates false measures of ultrasound attenuation. Further, the removal of all hair using both shaving and depilation cream is important, as remaining hair can trap air bubbles, which will cast shadows on B-mode images. Finally, as the presence of food in the stomach and intestines can obscure the liver, especially in normal chow-fed animals, adequate fasting of all animals is critical to successful imaging of the liver.

Although liver elasticity measurements from SWE and the HR index are valuable readouts to

assess liver fibrosis and steatosis in preclinical models of NASH, the technique has a few limitations. Factors such as inflammation, hepatic congestion, cholestasis, and outflow tract obstruction influence liver stiffness and thus, may influence the overall specificity of this technique in measuring liver fibrosis[8,14-16]. Similarly, brightness of the liver in B-mode ultrasound images can be influenced by fibrosis and thus, may affect the accuracy of the HR index in measuring steatosis. More studies are needed to clarify the contribution of these influencing factors on elasticity and steatosis and establish cut-off values for these readouts in different preclinical models of NASH. Further, this study did not evaluate the sensitivity of the HR index as a biomarker to assess liver steatosis in a preclinical efficacy study.

Measurement of liver stiffness using SWE has the potential to become a valuable tool for understanding the pathophysiology of NASH/NAFLD as well as for developing novel treatments for this condition. By allowing the researcher to determine both liver steatosis and tissue stiffness without the need for an invasive biopsy, animals in preclinical studies can be monitored longitudinally, and drug effects on individual subjects can be quantified over time.

ACKNOWLEDGMENTS:

The authors would like to thank the Pfizer Comparative Medicine Operations Team for their hard work caring for and ensuring the health of the study animals as well as assisting with some of the techniques. Also, thanks are owed to Danielle Crowell, Gary Seitis, Jennifer Ashley Traverse for their help with tissue processing for histological analyses. In addition, authors would like to thank Julita Ramirez for reviewing and providing valuable feedback during preparation of this manuscript.

DISCLOSURES:

All authors are employees of Pfizer, Inc.

REFERENCES:

1 Younossi, Z. M. et al. Global epidemiology of nonalcoholic fatty liver disease-Meta-analytic assessment of prevalence, incidence, and outcomes. *Hepatology.* **64** (1), 73–84 (2016).

2 Boland, M. L. et al. Towards a standard diet-induced and biopsy-confirmed mouse model of non-alcoholic steatohepatitis: Impact of dietary fat source. *World Journal of Gastroenterology.* **25** (33), 4904–4920 (2019).

3 Oldham, S., Rivera, C., Boland, M. L., Trevaskis, J. L. Incorporation of a survivable liver biopsy procedure in mice to assess non-alcoholic steatohepatitis (NASH) resolution. *Journal of Visualized Experiments: JoVE.* (146), 59130 (2019).

4 Bercoff, J., Tanter, M., Fink, M. Supersonic shear imaging: a new technique for soft tissue elasticity mapping. *IEEE Transactions on Ultrasonics, Ferroelectrics, and Frequency Control.* **51** (4), 396–409 (2004).

5 Bavu, E. et al. Noninvasive in vivo liver fibrosis evaluation using supersonic shear imaging: a clinical study on 113 hepatitis C virus patients. *Ultrasound in Medicine & Biology.* **37** (9), 1361–1373 (2011).

6 Ferraioli, G. et al. Accuracy of real-time shear wave elastography for assessing liver fibrosis in chronic hepatitis C: a pilot study. *Hepatology.* **56** (6), 2125–2133 (2012).

7 Ross, T. T. et al. Acetyl-CoA carboxylase inhibition improves multiple dimensions of NASH pathogenesis in model systems. *Cellular and Molecular Gastroenterology and Hepatology.* **10** (4), 829–851 (2020).
8 Gu, L. H., Gu, G. X., Wan, P., Li, F. H., Xia, Q. The utility of two-dimensional shear wave elastography and texture analysis for monitoring liver fibrosis in rat model. *Hepatobiliary & Pancreatic Diseases International.* **20** (1), 46–52 (2020).
9 Marshall, R. H., Eissa, M., Bluth, E. I., Gulotta, P. M., Davis, N. K. Hepatorenal index as an accurate, simple, and effective tool in screening for steatosis. *American Journal of Roentgenology.* **199** (5), 997–1002 (2012).
10 Webb, M. et al. Diagnostic value of a computerized hepatorenal index for sonographic quantification of liver steatosis. *American Journal of Roentgenology.* **192** (4), 909–914 (2009).
11 Tous, M., Ferre, N., Camps, J., Riu, F., Joven, J. Feeding apolipoprotein E-knockout mice with cholesterol and fat enriched diets may be a model of non-alcoholic steatohepatitis. *Molecular and Cellular Biochemistry.* **268** (1–2), 53–58 (2005).
12 Kirsch, R. et al. Rodent nutritional model of non-alcoholic steatohepatitis: species, strain and sex difference studies. *Journal of Gastroenterology and Hepatology.* **18** (11), 1272–1282 (2003).
13 2018 Scientific Program. *Journal of Ultrasound in Medicine.* **37** (S1), S1–S220 (2018).
14 Engelmann, G., Quader, J., Teufel, U., Schenk, J. P. Limitations and opportunities of non-invasive liver stiffness measurement in children. *World Journal of Hepatology.* **9** (8), 409–417 (2017).
15 Piscaglia, F., Salvatore, V., Mulazzani, L., Cantisani, V., Schiavone, C. Ultrasound shear wave elastography for liver disease. a critical appraisal of the many actors on the stage. *Ultraschall in der Medizin.* **37** (1), 1–5 (2016).
16 Singh, S., Loomba, R. Role of two-dimensional shear wave elastography in the assessment of chronic liver diseases. *Hepatology.* **67** (1), 13–15 (2018).

Figure 1

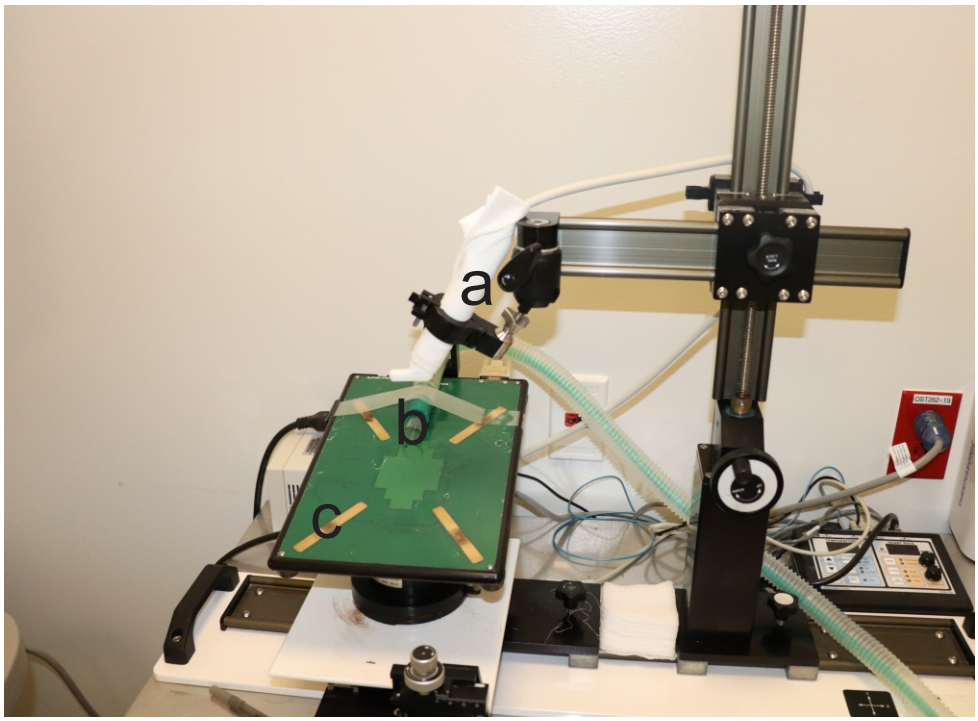

Figure 2

Click here to access/download;Figure;Fig 2 Revision.pdf

A

B

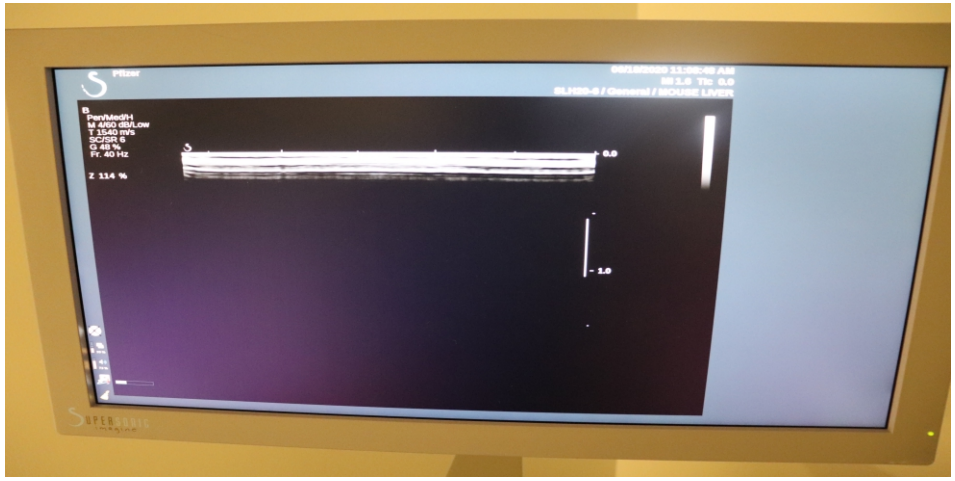

C

D

Figure 3

A

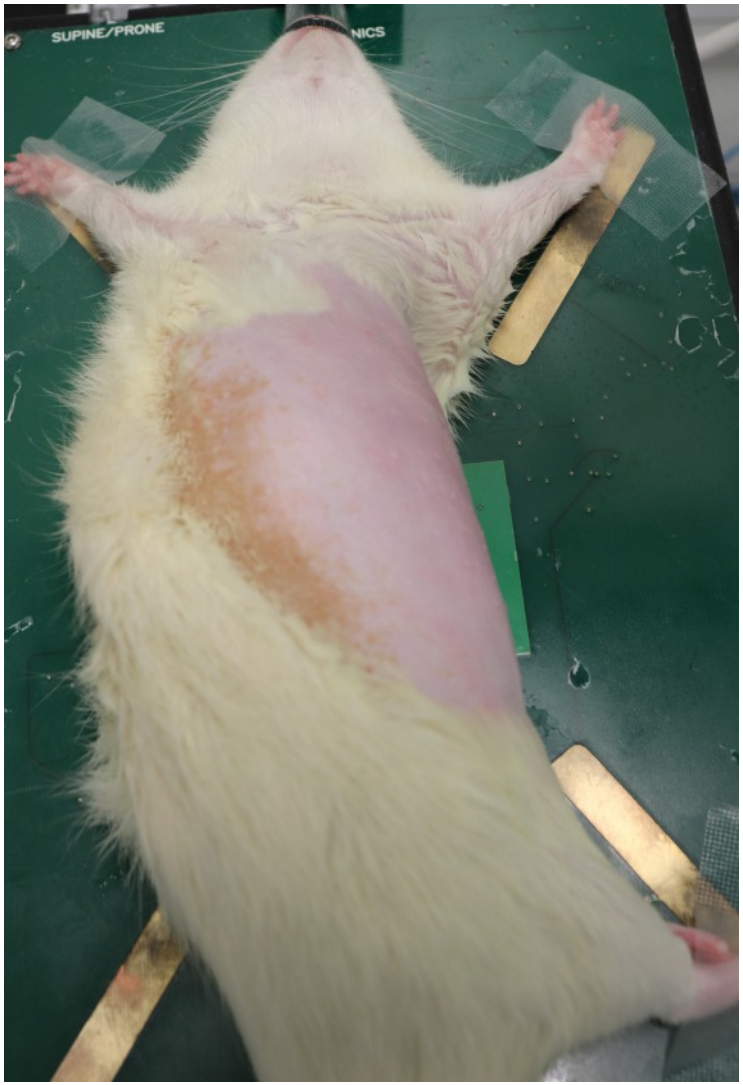

B

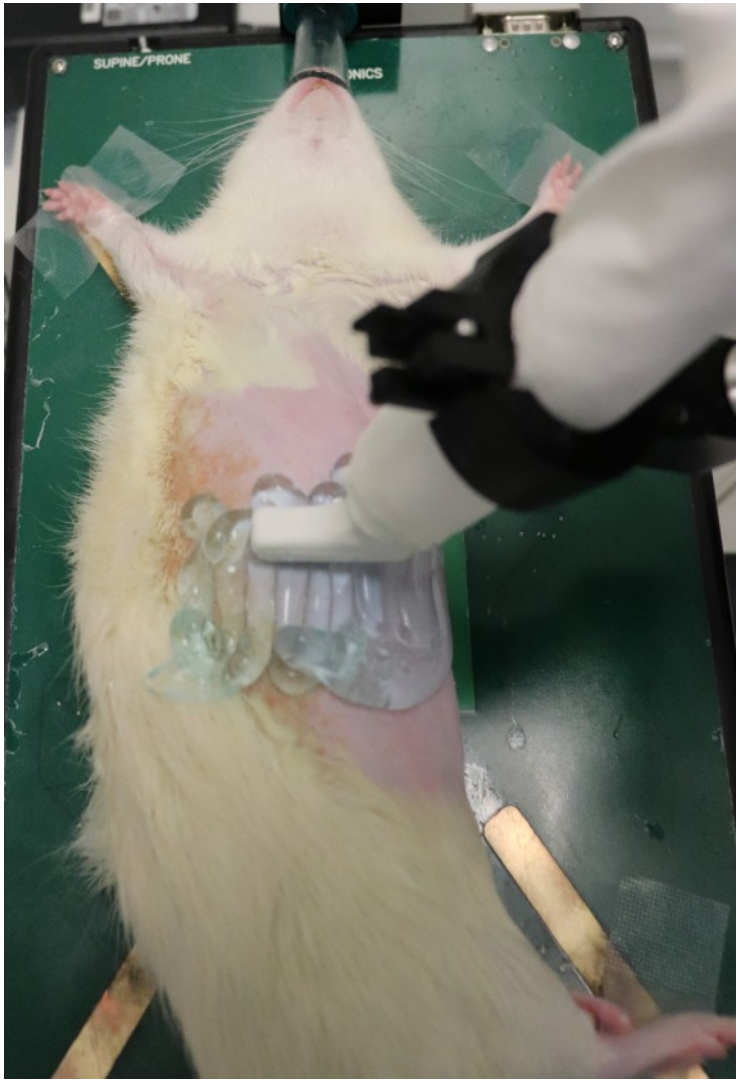

Figure 4

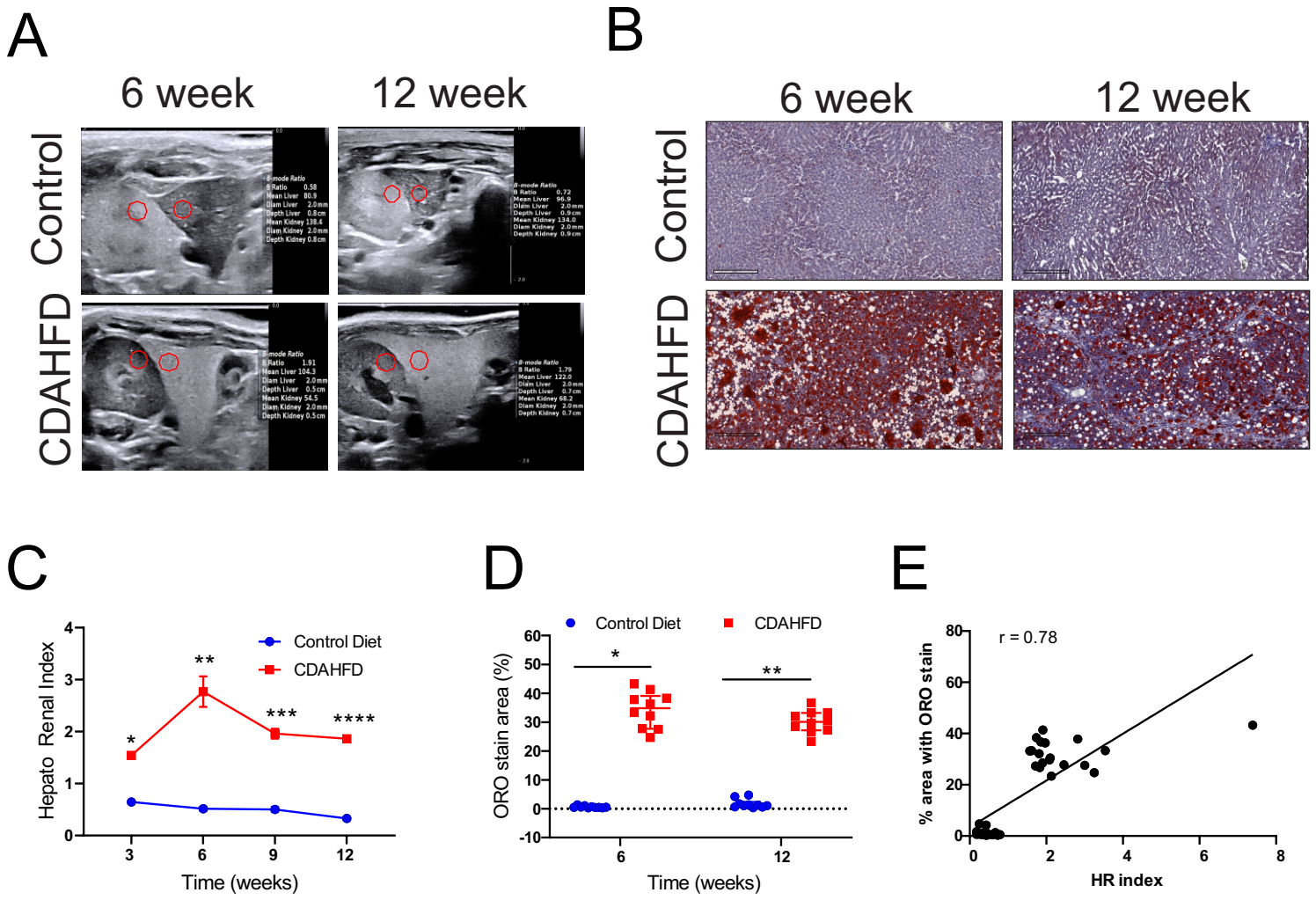

Figure 5

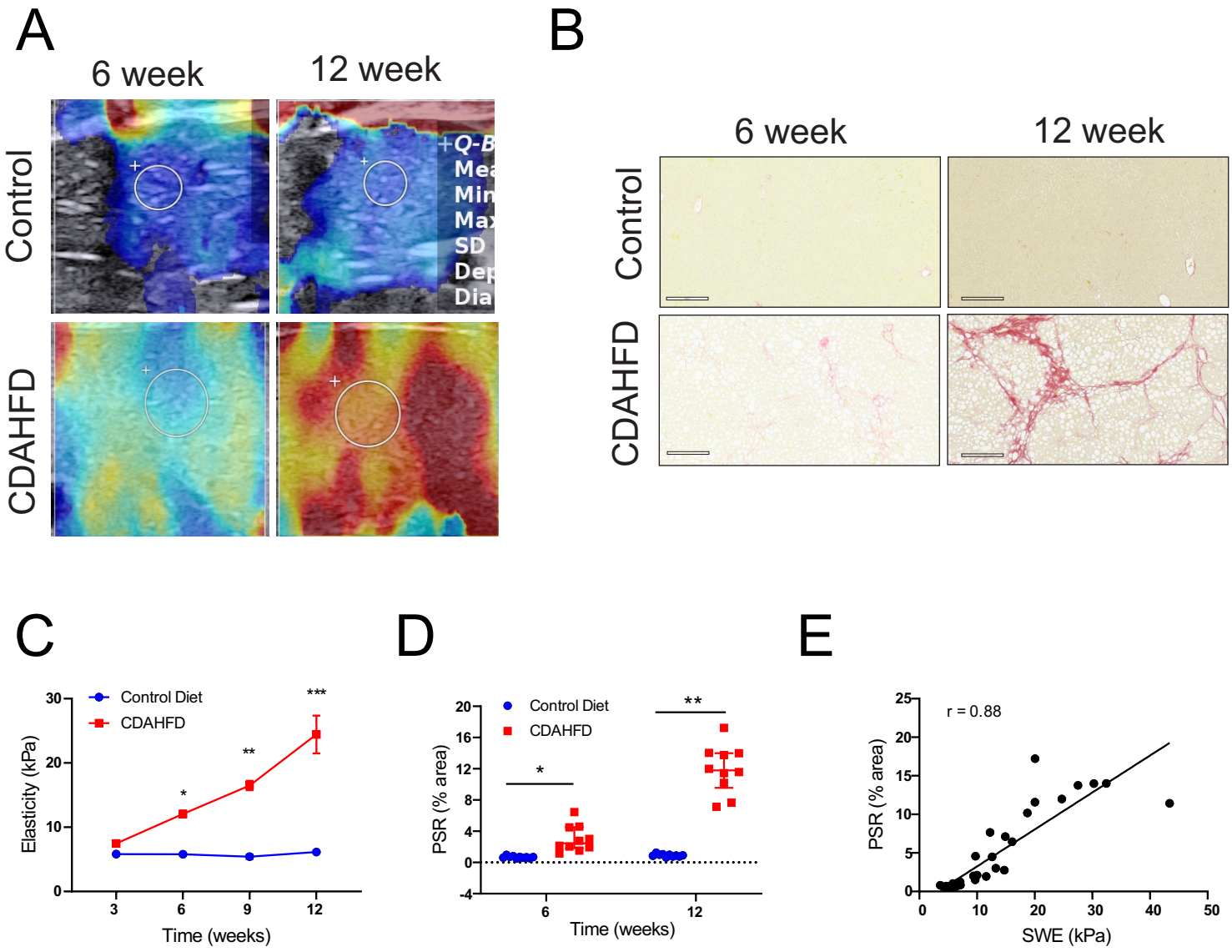

Name of Material/Equipment	Company	Catalog Number	
	Supersonic		
Aixplorer	Imagine		
Aixplorer SuperLinear SLH20-6	Supersonic		
Transducer	Imagine		
Alpha-dri bedding			
Aperio AT2 scanner	Leica Biosystems		
Compac 6 Anesthesia System	VetEquip		
Manage Imager Database	Leica Biosystems		
Mayer's Hematoxilin	Dako/Agilent		
Nair	Church & Dwight		
Oil Red O solution	Poly Scientific		
	Rowley		
Picrosirius Red Stain (PSR)	Biochemical	F-357-2	
	Dechra Veterinary		
Puralube Opthalmic ointment	Product		
	Sakura Finetek		
Tissue-Tek Prisma Plus	USA		
VISIOPHARM software	Visiopharm		
	Research Diets	A06071309i	
	Purina		5053
	Charles River		
Wistar Han rats	Laboratories		

Comments/Description

Shear Wave Elastography Instrument

Transducer for Shear Wave Elastography
rat cages
Digital Pathology Brightfield Scanner
Anesthesia Vaporizer and Delivery System. Any anesthesia delivery system can be used, however.
Digital Pathology
H&E Staining/Histology
Hair remover
Lipid Staining/Histology

Collagen Stain/Histology

Lubricatn to prevent eye dryness during anesthesia

Automated slide stainer
Digital pathology software
NASH inducing diet
Control animal chow

Editors
JoVE
Cambridge, MA 02140
December 12, 2020

Dear Editor,

I'm writing to submit our revised manuscript (JOVE JoVE62403) entitled, "Application of Ultrasound (US) and Shear Wave Elastography (SWE) Imaging in a Rat Model of NAFLD/NASH" for consideration as a JoVE Biology Methods video article. We addressed majority of reviewers and your comments in this revised version. Please see our rebuttal response in 'RED font' below.

Sincerely,
Dinesh Hirenallur-Shanthappa
Corresponding Author
Pfizer Inc
1 Portland Street
Cambridge, MA 02139

Editorial comments:

1. Please take this opportunity to thoroughly proofread the manuscript to ensure that there are no spelling or grammar issues.
2. Please revise the text to avoid the use of any personal pronouns (e.g., "we", "you", "our" etc.).
3. JoVE cannot publish manuscripts containing commercial language. This includes trademark symbols (™), registered symbols (®), and company names before an instrument or reagent. Please remove all commercial language from your manuscript and use generic terms instead. All commercial products should be sufficiently referenced in the Table of Materials.
For example: Purina LabDiet, Supersonic Imagine, Aixplorer, Fujifilm VisualSonics Imaging Station, etc.
4. Line 127: Please specify the inhalant used for anesthesia. Please include the details regarding the concentrations used for induction and maintenance.
5. Line 160/162/164: For time units, please use abbreviated forms for durations of less than one day when the unit is preceded by a numeral. Do not abbreviate day, week, month, and year.
Examples: 5 h, 10 min, 100 s, 8 days, 10 weeks
6. Please include a one-line space between each protocol step and highlight up to 3 pages of the Protocol (including headings and spacing) that identifies the essential steps of the protocol

for the video, i.e., the steps that should be visualized to tell the most cohesive story of the Protocol. Remember that non-highlighted Protocol steps will remain in the manuscript, and therefore will still be available to the reader.
7. Please move the Figure Legends section to the end of the Representative Results section.
8. Figure 1: Please remove any commercial content from the Figure/ Figure legend. Please use generic terms instead.
9. Figure 2: Please consider removing the image and replacing it with an image that does not contain any commercial content. JoVE cannot publish manuscripts containing commercial language. This includes trademark symbols (™), registered symbols (®), and company names before an instrument or reagent.

Authors Response to Editor Comment: Thanks for reviewing the article suggesting changes. We made all recommended changes to the manuscript.

Reviewers' comments:

Reviewer #1:

Manuscript Summary:

Thank you very much for the opportunity to review this well written and interesting manuscript. Moring et al. describe the application of Ultrasound and Shear Wave Elastography Imaging in a longitudinal assessment of steatosis and fibrosis in pre-clinical animal model. There is indeed an unmet need for a reliable, reproducible assessment method for progression of liver disease in NAFLD/NASH animal models that does not involve terminal collection of organs or a liver biopsy. This imaging method is described in detail and some preliminary data on the correlation of their model with histology, the current gold standard, is provided. However, the experimental part of the manuscript severely lacks in detail and is insufficient in its current form. A few major points need to be addressed by the authors before this manuscript can be published.

Major Concerns:

1. Why did the authors choose a rat model instead of the more commonly used mouse model for NAFLD/NASH? Could the authors comment on this crucial point and a potential applicability of the methods used to a mouse model?

Authors Response:

We have performed experiments to validate the shear wave elastography (SWE) imaging application to assess the NAFLD/NASH phenotype in both mouse and rat models. Validation results in both the rat and mouse are very similar. Notably, the mouse validation part of the data has been considered for a different publication and was also presented at the AIUM 2018 meeting (Swanson T et al, 2018 Scientific Program. J Ultrasound Med, 37: S1-S220. https://doi.org/10.1002/jum.14750). The SWE liver imaging approach is similar between mice and rats. In the revised manuscript, we have added the following statement to clarify: "As in the rat NASH model, SWE imaging in the CDAHFD-–induced NASH mouse model showed excellent correlation between liver elasticity values and percent of PSR positive staining area in liver (internal unpublished results). Thus, SWE can be a valuable tool to assess liver fibrosis in both rat and mouse preclinical models of NAFLD/NASH."

2. Details about the animals used is completely absent in the manuscript. Could the authors outline what strain they used, how old the animals were, how many animals they used per group, how they were housed (SPF?) etc.?

The requested information has been updated under protocol section 1 on page # 4 and 5.

3. At what age of the animals was the experimental diet started?

Rats were placed on the special diet about 6 to 7 weeks old. This is based on standard weight vs growth curve data for Wistar Han rats. We updated this information under protocol section 1.

4. Generally a simple figure outlining the experimental setup would help in better understanding the protocol used.

I agree with the reviewer's suggestion that a schematic of the experimental set up would be helpful. However, since detailed steps are incorporated in the written version and there will be a video describing the imaging method as well as image acquisition and steps, we think that it may be redundant.

5. Results: What statistical tests were used for the analysis of the data? The authors provide significant levels in their figures but do not mention p-values. Please also provide the mean H:R index for the two groups in the results section.

Information about the statistical tests used has been added under protocol section 8. Also, added mean H:R index values have been added in the results section.

6. Figure 4, Figure 5: Please also provide representative pictures of the liver histology to be correlated with the ultrasound imaging for Oil Red and Picro Sirius Red stainings respectively.

Figures 4 and 5 have been updated with representative PSR and ORO-stained histology of the liver.

7. Methodological details on the histological analysis is lacking.

We have now included detailed description of the ORO and PSR staining in the protocol section under 7.

8. Introduction, page 4, line 89: Could the authors discuss the already existing literature on the topic more in detail and comment how their model and technique is to be seen in this context?

The existing literature lacks detailed technique and methodology information on the application of SWE imaging in preclinical models of NASH. We have now included this statement in the introduction to the revised manuscript (page # 3, line 93, 94). To clarify, we have also stated the main goal of the manuscript in the last paragraph of the introduction (line # 102).

9. Protocol, Page 9, line 239: How big was the difference between the individual measurements? Was there a difference in the results if the author took 3 or 5 different measurements?

In this study we acquired only 3 images at each time point for B-mode and SWE images to calculate HR and elasticity. We updated this information in the protocol section 4.5. However, in the past we have compared the average H:R index and SWE values using 3 to 5 images per time point in a mouse study and observed negligible differences in the average values of these readouts. For example, the average elasticity values calculated from 3 and 5 images are 5.77 ± 1.10 and 5.68 ± 0.96, respectively, in a control group. Similarly, the average elasticity values calculated from 3 and 5 images at the 12-week time point in CDAHFD mice are 10.94 ± 1.43 and 11.09 ± 1.41, respectively.

10. Protocol, Page 9, line 259: it is unclear what software was used to retrieve the "B Ratio" number and the "Q Box" and what it exactly refers to. It would be helpful to the reader if the authors could comment on these points.

We used a tool built into the ultrasound system software in order to measure the elasticity of the liver for the ROI. Similarly, the B-mode ratio is measured using a built-in tool that measures the ratio of renal to liver tissue brightness. We made edits in the protocol section to clarify this.

11. Could the authors provide a rough estimate of the costs involved with the equipment? This would be a major help for research groups to decide if they are able to implement the imaging methods described in this manuscript.

Multiple companies manufacture ultrasound equipment with the capability for shear wave elastography. The authors believe that listing the price of SWE equipment is outside the scope of this manuscript.

12. Discussion, page 13, line 341: The authors take their conclusion one point too far. These surrogate markers ARE already used in clinical practice today. The authors provided a protocol for application of the techniques in laboratory animals not the other way around.

We agree with the reviewer and have made the appropriate changes to the conclusion of the manuscript.

13. A limitations section is generally missing. Could the authors comment on the limitations of their imaging method? What are potential obstacles to a widespread implementation of US imaging for assessment of liver injury in NAFLD/NASH models?

We have added a paragraph in the discussion section to highlight limitations of these imaging methods for assessing NAFLD/NASH in preclinical models (line # 560 to 569).

Reviewer #2:
Manuscript Summary:
It is with great pleasure that I receive the paper entitled "Application of Ultrasound and Shear Wave Elastography Imaging in a Rat Model of NAFLD/NASH" to review. I see commitment from authors with scientific method and a great work done.
Authors propose the combination of two non-invasive techniques to evaluate the progression of liver injury in murine using pro-NASH diet compared to normal chow. They used Ultrasound 2D Imaging for fat accumulation analysis, through hepatorenal index (HR), and Shear Wave Elastography (SWE) for fibrotic establishment evaluation. Data obtained from imaging was comparable to golden standard histological Liver Biopsy staining with great positive correlation. Data demonstrate the aggravation of NAFLD/NASH from 3 to 12 weeks of induction.

Major Concerns:

Hepatorenal (HR) index is criticized in clinic, but in combination with other parameters it can provide robust data on the establishment and progression of steatosis in the liver. This study shows a clear increase in HR index from 3 to 12 weeks of induction, demonstrating the worsening of steatosis. However, the figure representing the normal HR index does not appears to reproduce data described in text [B ratio = 0,43 in Figure4A (3 weeks) instead of "close to 1", cited in line 271].

We agree with the reviewer's comment that the HR index should be close to 1. However, we noticed that liver brightness in control rats was consistently lower than the brightness of the kidney cortex on B-mode images. As a result, we observed an average HR index ranging from average

of 0.5 to 0.7 in control rats. To reflect this observation, we edited the results section to add the mean H:R index of control rats and selected different representative images for Figure 4A.

SWE is one of the emerging techniques that can support clinical investigation of liver injuries. However, literature suggests that SWE sensibly differentiate between severe instead of significant fibrosis. Authors must emphasize that since the induction protocol is intimately related to degree of the injury. Should say more; It has already been cited that different conditions such as inflammation, outflow tract obstruction and congestion of the liver can alter organ's stiffness, leading to biased data. In addition, different etiologies have different cut-off values for stiffness.

The reviewer correctly mentions some important limitations of SWE. We have thus added a paragraph in the discussion to outline these limitations of the SWE technique for assessing liver fibrosis and mentioned the requirement for additional studies to establish cut-off values for SWE and HR indices in different preclinical models of NAFLD/NASH.

The use of automatic TGC requires attention because 2D Gain is linked to the US signal received and can interfere with image brightness, masking real information. It could be interesting to investigate the establishment of a 2D Gain value with small deviation.

We agree that 2D gain is linked to the US signal that is received, which can interfere with image brightness when one uses the auto TGC. It would be interesting to further investigate the effect of 2D gain on the HR index. However, since we measured brightness of the renal cortex and liver parenchyma on the same B-mode image at the same tissue depth and the HR index is expressed as a ratio of these measurements, using automatic TGC likely has a negligible effect on the final HR index readout. Thus, we have not further investigated the effects of 2D gain values.

Minor Concerns:
Monitoring of NAFLD is extremely important, since this pathology emerges as a silent, costly economically and dangerous disease worldwide. I must agree that the possibility of using a non-invasive technique for stratification of hepatic diseases is necessary in clinic. Invasive puncture of the liver is until now the most widely used technique so far, and I understand it is sometimes extremely necessary, but the improvement that is present today in Clinical Imaging Technology is fundamental and necessary to avoid diagnosis through invasive procedures. It is important to emphasize that SWE is a powerful technological resource in follow-up studies. Serial comparison of multiple time-points certainly can demonstrate the progression of the disease.

Thanks for recognizing the value of SWE on assessing liver fibrosis in the clinical and preclinical NASH field. In our concluding paragraph, we have stressed the robustness of this technology and advantages of using this tool to assess disease progression in a longitudinal fashion.